LBL-29305

Lawrence Berkeley Laboratory
UNIVERSITY OF CALIFORNIA

Materials & Chemical Sciences Division

Presented at the ACS Symposium entitled "50th Anniversary of the Discovery of Transuranium Elements," Washington, DC, August 26–31, 1990, and to be published in the Proceedings

Magnetic and Optical Properties of Np and Pu Ions and Compounds

N.M. Edelstein

August 1990

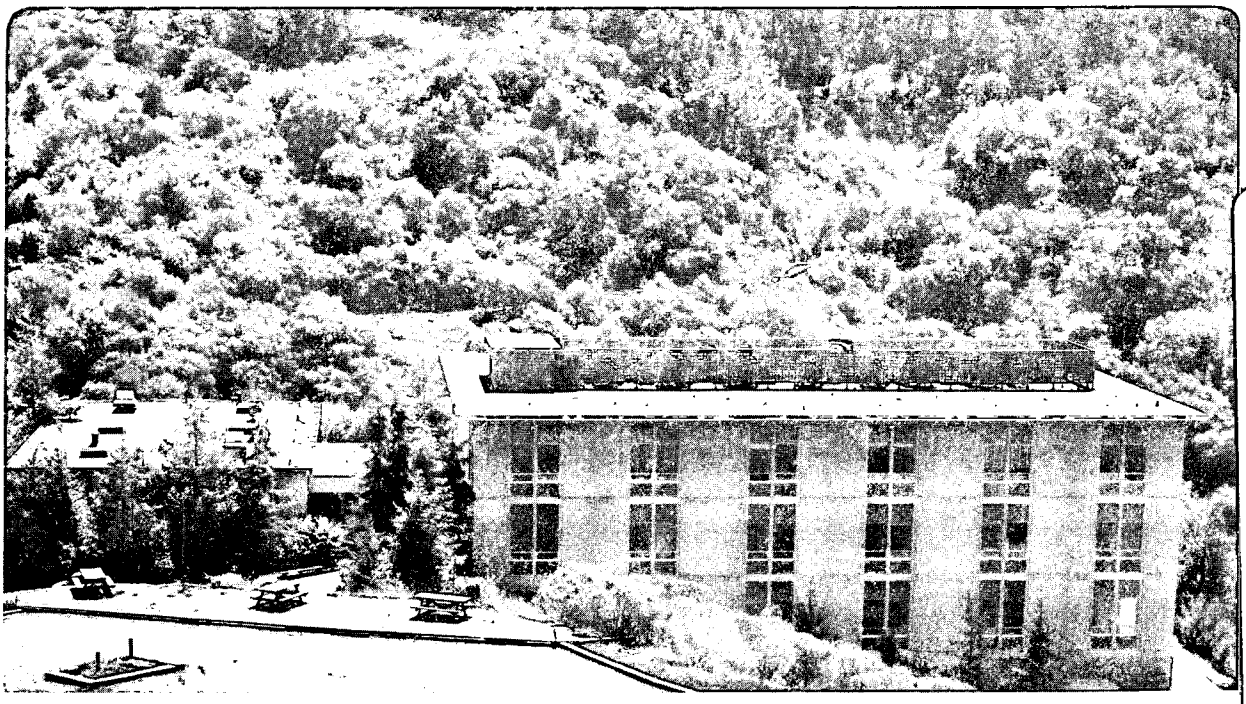

LOAN COPY
Circulates
for 2 weeks
Bldg. 50 Library.
LBL-29305
Copy 2

Prepared for the U.S. Department of Energy under Contract Number DE-AC03-76SF00098.

DISCLAIMER

This document was prepared as an account of work sponsored by the United States Government. While this document is believed to contain correct information, neither the United States Government nor any agency thereof, nor the Regents of the University of California, nor any of their employees, makes any warranty, express or implied, or assumes any legal responsibility for the accuracy, completeness, or usefulness of any information, apparatus, product, or process disclosed, or represents that its use would not infringe privately owned rights. Reference herein to any specific commercial product, process, or service by its trade name, trademark, manufacturer, or otherwise, does not necessarily constitute or imply its endorsement, recommendation, or favoring by the United States Government or any agency thereof, or the Regents of the University of California. The views and opinions of authors expressed herein do not necessarily state or reflect those of the United States Government or any agency thereof or the Regents of the University of California.

LBL-29305

MAGNETIC AND OPTICAL PROPERTIES OF Np AND Pu IONS AND COMPOUNDS

Norman M. Edelstein

Materials and Chemical Sciences Division

Lawrence Berkeley Laboratory

University of California

Berkeley, California 94720

This work was supported by the Director, Office of Energy Research, Office of Basic Energy Sciences, Chemical Sciences Division of the U.S. Department of Energy under Contract No. DE-AC03-76SF00098.

LBL-29305

MAGNETIC AND OPTICAL PROPERTIES OF Np AND Pu IONS AND COMPOUNDS

Norman M. Edelstein

Materials and Chemical Sciences Division

Lawrence Berkeley Laboratory, Berkeley, California 94720

Abstract

Three topics are reviewed in this paper. They are the magnetic and optical properties of NpF_6 and PuF_6, $Np(BH_3CH_3)_4$, and the hyperfine anomaly of $^{239,241}Pu$. Based on recent optical data of NpF_6 and PuF_6 in Ar matrices, new crystal field analyses of these molecules are presented. The temperature dependent ^1H and ^{11}B NMR shifts of $Np(BH_3CH_3)_4$ are discussed.

Introduction

The magnetic and optical properties of Np and Pu ions encompass a wide variety of measurements and materials. In this paper three topics are chosen as examples of some of the studies that have been conducted. The first topic is a review of the electronic structure studies of NpF_6 and PuF_6. Recently, new data have been obtained on these molecules diluted in argon matrices. With this new information, an updated analysis of the optical and magnetic data is given.

The second topic is a review of the physical, magnetic, and optical properties of $Np(BH_3CH_3)_4$. This molecule possesses high symmetry about the Np^{4+} ion (T_d) which simplifies the analysis of the optical and magnetic data. The results of this analysis are used to interpret recent NMR measurements (as a function of temperature) on ^1H and ^{11}B in $Np(BH_3CH_3)_4$.

The third topic is a review of earlier work on the hyperfine anomaly between $^{239,241}Pu$. This topic was chosen because it is an excellent example of the effects of relativity in the heaviest elements.

Actinide Hexafluorides

The actinide hexafluorides, MF_6 (M = U, Np, Pu) are volatile molecular solids at room temperature. Because of their important industrial applications, their chemical properties have been extensively studied (1). Their electronic structure has also been the subject of a number of experimental investigations both in the gas phase and in the solid state. For NpF_6 the solid state measurements include magnetic susceptibility measurements as a function of temperature both in the pure compound and diluted in the isomorphorus, weakly temperature independent paramagnet, UF_6 (2-3). In addition, the electron paramagnetic resonance (EPR) spectrum and a detailed study of the fluorine superhyperfine structure by electron-nuclear double resonance (ENDOR) methods have been reported (4-5).

Optical spectra due to electronic transitions within the $5f^1$ configuration were first reported by Goodman and Fred (6). For a $5f^1$ electron in octahedral symmetry, four electronic transitions between the ground level and the four excited levels should be observed. Goodman and Fred reported two band systems (in the gas phase) in the near-infra red region and two more band systems in the ultra-violet region. These latter bands were partially obscured by an ultra-violet absorption edge. Because of the octahedral symmetry about the Np^{6+} ion, the electronic transition is not observed via an allowed electron dipole transition, but becomes partially allowed when accompanied by the absorption or emission of a phonon of odd (ungerade) symmetry. For some transitions, the band may be observed via a magnetic dipole transition. The magnetic and optical data for NpF_6 have been analyzed by a number of groups (4), (6-7) with the most detailed calculations given by Eisenstein and Pryce (7). The results of these analyses are very similar.

The only magnetic data for PuF_6 were reported by Gruen, et al. (8) The gas phase absorption spectrum of PuF_6 was first published by Steindler and Gunther (9). Subsequently, Kugel et al.(10) examined various regions of the PuF_6 spectrum by a high resolution laser technique. Recently, the Los Alamos group has reexamined the optical spectra of both NpF_6 and PuF_6 as isolated molecules in a solid argon matrix at low temperatures using both absorption and fluorescence techniques (11-12). The analyses of the optical data has verified some earlier electronic assignments and given more accurate values for the energy levels.

A number of theoretical calculations have been published which have analyzed the electronic structure of the MF_6 (M = U, Np, Pu) compounds (13-15). The most recent *ab initio* calculation by Wadt gave a calculated electronic spectrum for the $5f^2$ configuration of PuF_6 in good agreement with the Los Alamos experimental data (13). Earlier work by Boring and Hecht (14) and Kugel et al. (10) included crystal field analyses of the PuF_6 data based on the data available at the time. With the new optical data available from the Los Alamos experiments, a reanalysis of this data is presented here for NpF_6 and PuF_6 based on the classical crystal field model.

Analysis of NpF_6 Data

The Hamiltonian used to describe one f electron in an octahedral crystal field is:

$$\mathcal{H} = \mathcal{H}_{SO} + \mathcal{H}_{CF}$$

where

$$\mathcal{H}_{SO} = \zeta_{5f}\vec{\ell}\cdot\vec{s}$$

and

$$\mathcal{H}_{CF} = B_0^4[C_0^4 + (\tfrac{5}{14})^{1/2}(C_{-4}^4 + C_4^4)] \qquad (1)$$

$$+ B_0^6[C_0^6 - (\tfrac{7}{2})^{1/2}(C_{-4}^6 + C_4^6)].$$

There is one free ion parameter ζ_f representing the radial part of the spin-orbit coupling constant. The crystal field interaction for O_h symmetry is represented by two parameters B_0^4 and B_0^6 and the tensor operators C_q^k. The crystal field parameters may alternatively be written as shown in Table 1. Figure 1 shows the labelling of the states and the relative energy levels of one f electron as a function of the ratio of the spin-orbit coupling vs. the crystal field interaction.

Mulford et al.[12] reported the $\Delta E(\Gamma_7 \rightarrow \Gamma_8)$ transition of NpF_6 at 7610 cm^{-1} and the $\Delta E(\Gamma_7 \rightarrow \Gamma_7')$ transition at 9366 cm^{-1} (12). These values are very similar to the energies used by Eisenstein and Pryce. Following earlier work, the g value of the ground Γ_7 state, g = -0.6052 (5), fixes the ratio of $\zeta/\Delta E(\Gamma_7'-\Gamma_7)$. Since the energy difference $\Delta E(\Gamma_7'-\Gamma_7)$ is known, the spin-orbit coupling constant ζ is immediately determined. From the value of $\Delta E(\Gamma_8-\Gamma_7)$ the remaining crystal field parameter may be evaluated. The experimental and calculated spectra for NpF_6 are shown in Table 2 and the Hamiltonian parameters are given in Table 3. The calculated values of the reciprocal magnetic susceptibility vs. temperature are compared with some of the experimental data of Hutchison and Weinstock (4) in Figure 2.

Analysis of the PuF6 Optical Spectrum

Wadt (15) has given a table (Table VII in his paper) which presents the results of a number of types of calculations plus the experimental data for PuF_6 isolated in an argon matrix of Dewey, et al. (11). In the following, the assignments of Dewey, et al. (11) as listed by Wadt are used.

The Hamiltonian for the $5f^2$ configuration in a crystal field of O_h symmetry is written as (16):

$$\mathcal{H} = \mathcal{H}_{FI} + \mathcal{H}_{CF},$$

where

$$\mathcal{H}_{FI} = \sum_{k=0,2,4,6} f_k F^k(nf,nf) + \zeta_f a_{so} + \alpha L(L+1)$$

$$+ \beta G(G_2) + \gamma(R_7) + \sum_{k=0,2,4} m_k M^k + \sum_{k=2,4,6} p_k P^k \tag{2}$$

and $\mathcal{H}_{CF}$ is as given before for the f^1 case (Eq. 1). The $F^k(nf,nf)$'s and ζ_f represent, respectively, the radial parts of the electrostatic and spin-orbit interactions between f electrons, while f_k and a_{so} are the angular parts of the interactions. α,β, and γ are the parameters associated with the two-body effective operators of configuration interaction. The M^k parameters represent the spin-spin and spin-other-orbit interactions while the P^k parameters arise from electrostatic-spin-orbit interactions with higher configurations.

Table 4 presents Hamiltonian parameters for the $5f^2$ configuration from analyses of the U^{4+} free ion (17), the molecular compound $U(BD_4)_4$ (16), and the results of a Hartree-Fock calculation for the U^{4+} and Pu^{6+} free ions obtained with Cowan's program (18). It is expected that the crystal field will differ only slightly between NpF_6 and PuF_6. Accordingly, only the free ion parameters F^2, F^4, F^6, and ζ initially were allowed to vary in the fit to the energy levels of PuF_6, and the crystal field parameters were set at the values found for NpF_6 (Table 3). After the best fit was found for these free ion parameters, the above set plus B_0^4 and B_0^6 were treated as free parameters. It was found that the free ion parameters plus B_0^4 and B_0^6, when allowed to vary together, converged fairly rapidly. The fit was slightly better with the configuration interaction parameters, the M^k's, and P^k's fixed at the U(V) free ion values than if these parameters were set to zero. The adjusted parameters are shown in Table 4 (PuF_6(A)) and the calculated and experimental energy levels are given in Table 5. As others have found the fit could be markedly improved by switching the assignments of the $2\Gamma_3$ and $2\Gamma_5$. The parameters found with these assignments are shown in the PuF_6(B) column of Table 4 and the calculated energies are shown in the Calc. B column of Table 5. The calculated value of the temperature independent paramagnetism (TIP) in the 2-300K range is 272 x 10^{-6} emu/mole. Both calculations A and B gave the same result. This number is in reasonable agreement with

the only magnetic measurements on PuF_6 by Gruen et al. who obtained the values 173 x 10^{-6} emu/mole and 131 x 10^{-6} emu/mole at 295K and 81K, respectively (8).

The "free ion" parameters obtained from the fit are quite strange. First of all F^2 is reduced by greater than 50% from its Hartree-Fock value and F^4 is larger than the calculated Hartree-Fock value. The empirical values for F^6 and ζ seem to be of reasonable magnitude when compared to the Hartree-Fock values and the usual trends of the "free ion" parameters found in crystals. Note, however, that the crystal field is approximately 20 times larger than found in $U(BD_4)_4$ and approximately 6 times larger than for the UCl_6^{2-} anion (19). Thus the PuF_6 molecule represents a severe test of the parametric theory. Because it is a parametric theory, the adjusted parameters may include interactions which have not been explicitly considered in the formulation of the Hamiltonian. However, it is reassuring that the crystal field parameters do not change drastically from those of NpF_6 when allowed to freely vary with the "free ion" parameters. Perhaps a better model for comparison with the empirical parameters of PuF_6 would be d transition metal compounds, where the magnitudes of the crystal field are similar to PuF_6, rather than other 5f compounds.

Clearly, more experimental studies are needed to obtain absorption and emission data for the higher-lying energy levels of both PuF_6 and NpF_6. The most favorable system to study would be NpF_6 (PuF_6) diluted in single crystals of UF_6. A detailed description of the method used to obtain such crystals has been given in the ENDOR paper by Butler and Hutchison (5). This system would have an added advantage since the site symmetry at the U site (assuming NpF_6 and PuF_6 substitute for a UF_6 molecule) is actually quite low. Butler and Hutchison (5) point out that tetragonal symmetry is a better approximate description for the UF_6 molecule in single crystals rather than octahedral symmetry. Thus it is possible that more forced electric dipole transitions will be observed in single crystals of $U_{1-x}M_xF_6$ (M = Np or Pu) than in the gas phase or as isolated molecules of NpF_6 or PuF_6 in an argon matrix.

Actinide Borohydrides

Uranium and thorium borohydrides, $An(BH_4)_4$ (An = Th, U), were first synthesized during the Manhattan project by the reaction (20-21)

$$AnF_4 + 2A\ell(BH_4)_3 \rightarrow An(BH_4)_4 + 2A\ell F_2BH_4.$$

These materials are polymeric in the solid state, and $Pa(BH_4)_4$, which has been synthesized by the same reaction as above, has a similar structure (22). The first three actinide borohydrides are volatile solid compounds at or near room temperature, with their vapor pressures increasing smoothly from $Th(BH_4)_4$ to $U(BH_4)_4$. $Th(BH_4)_4$ sublimes at 120°C, $U(BH_4)_4$ sublimes slowly at room temperature, and $Pa(BH_4)_4$ can be sublimed at 55°C. Np and Pu borohydrides also may be synthesized by the same reaction from their tetrafluorides. However they are volatile liquids at room temperature (melting points 14.2°C and 15°C, respectively) and are monomeric compounds in the solid state. Their physical properties more closely resemble those of Zr or Hf borohydrides, i.e. $Zr(BH_4)_4$, than of the first three actinide borohydrides (22).

Uranium borohydride may be studied as a monomeric species by dissolution in a hydrocarbon or by dilution as an impurity in a single crystal of Zr or Hf borohydride. $U(BH_4)_4$, as a monomeric species, has 12H atoms (three from each BH_4^- group) about the U^{4+} ion and the point group symmetry at the metal ion is T_d. Thus, the crystal field interaction in a parametric Hamiltonian depends only on two parameters. Bernstein and Keiderling discovered these methods and exploited them in a pioneering, high-resolution optical study of $U(BD_4)_4$ diluted in $Hf(BD_4)_4$ (23). Subsequently, the data of Bernstein and Keiderling were reanalyzed by Rajnak, et al. who also reported and fit the magnetic susceptibility data of the $U(BH_3CH_3)_4$, a molecule whose electronic structure closely resembles that of the monomeric $U(BH_4)_4$, but whose solid state structure is monomeric (24).

$U(BH_3CH_3)_4$ was first synthesized by Schelsinger, et al. by the reaction (25)

$$U(BH_4)_4 + \text{excess } B(CH_3)_3 \rightarrow U(BH_3CH_3)_4.$$

Shinomoto, et al. subsequently found the following reaction works satisfactorily:

$$MCl_4 + 4LiBH_3CH_3 \xrightarrow{\text{chlorobenzene}} M(BH_3CH_3)_4 + 4LiCl$$

where M = Zr, Hf, Th, U, and Np. All the metal methyltrihydroborates are volatile solids, may be sublimed under vacuum, and are soluble in non-coordinating hydrocarbons. X-ray structure analysis has shown that all the above $M(BH_3CH_3)_4$ compounds are monomeric in the solid-state and have T_d symmetry about the metal ion (26).

The optical spectrum of $Np(BD_4)_4$ diluted in $Zr(BD_4)_4$ was obtained and analyzed by Rajnak, et al. (27). EPR data have been obtained for $Np(BD_4)_4/Zr(BD_4)_4$, $Np(BH_3CH_3)_4/Zr(BH_3CH_3)_4$, and $Np(BH_3CH_3)_4$ diluted in methylcyclohexane. In addition, the magnetic susceptibility of pure $Np(BH_3CH_3)_4$ has been measured from 5 to ~ 300 K. On the basis of the analysis of the optical data of $Np(BD_4)_4$ the magnetic susceptibility data for $Np(BH_3CH_3)_4$ and the g values for $Np(BD_4)_4$ and $Np(BH_3CH_3)_4$ could be fit with the use of an orbital reduction factor (27). The values found are shown in Table 6. Note that in order to fit the $Np(BH_3CH_3)_4$ magnetic data a smaller value of the orbital reduction factor was used than for $Np(BD_4)_4$. This is indicative of increased covalency for the methyl compound compared to $Np(BD_4)_4$.

The EPR data for $Np(BD_4)_4$ and $Np(BH_3CH_3)_4$ showed no superhyperfine structure; that is the delocalization of unpaired spin density from the Np ion was not large enough at the ligand atoms to be resolved in the EPR experiment. Another way to obtain the same type of information is from an NMR experiment. Kot (28) recently measured the ^1H and ^{11}B NMR spectra of the BH_3CH_3 groups in $Np(BH_3CH_3)_4$ as a function of temperature. This data can be qualitatively analyzed using the electronic structure information obtained from the optical analysis of Rajnak, et al. (27). A similar analysis has been given for the temperature-dependent NMR spectra of $U(BH_3CH_3)_4$ (29). The data are shown as a function of 1/T in Figure 3. The high molecular symmetry (T_d) about the Np^{4+} ion in $Np(BH_3CH_3)_4$ is important because all pseudo-contact (dipolar) shifts are zero. Thus all observed NMR shifts are due to spin-transfer mechanisms.

The paramagnetic shifts, shown in Fig. 3, are measured relative to a similar diamagnetic reference, in this case $Th(BH_3CH_3)_4$. The units of the paramagnetic shift are in ppm, and shifts to higher field are defined as positive as given by Gamp, et al. (29). The theory of Kurland and McGarvey (30) has been used to analyze these shifts and summary of the relevant theory is given by Gamp, et al.

There are two basic mechanisms whereby unpaired spin from the metal ion (for f electron systems) can be transferred to the ligand atoms. The polarization mechanism transfers spin from the outer metal s and p orbitals to the ligand orbitals with the net result that the transferred spin has opposite sign to that of the f shell. The second mechanism involves a direct covalent transfer of spin from the ligand into the f shell. This second mechanism can result in either upfield or downfield shifts depending upon the detailed interactions for a particular system.

Gamp, et al., following Baker (31), assumed that for the polarization mechanism the isotropic shift should be proportional to the net spin in the f orbitals which is easily calculated from the same model used to fit the magnetic susceptibility. Thus

$$\Delta H/H = (K/g_N\beta_N)\,\langle S_z\rangle/H \qquad (3)$$

where $\langle S_z\rangle$ is the average total electronic spin, $\Delta H/H$, the shift in ppm, K a parameter proportional to the hyperfine coupling constant A, g_N, the nuclear g value for a particular nucleus, β_N, the nuclear magneton, and H the magnetic field. This equation is the same as the usual contact shift equation except A has been replaced by K. Values of $\langle S_z\rangle/H$ at a particular temperature have been calculated based on the model used to fit the temperature dependence of the magnetic susceptibility of $Np(BH_3CH_3)_4$. The parameter K in Eq.3 was then evaluated by a least-squares fit of the data. Since all the NMR data are referenced to $Th(BH_3CH_3)_4$, the intercept as $1/T = 0$ was set at 0. The best fit lines are shown in Fig. 3. The values of the parameter K and the standard deviations of the fits are shown in Table 7. The fits are quite good for the bridging and methyl protons, but deviate significantly for the ^{11}B data.

These results are very similar to those reported for $U(BH_3CH_3)_4$ and the conclusion is the same. For the bridging and methyl protons of $Np(BH_3CH_3)_4$, the polarization mechanism appears to be adequate to explain the NRR shifts; for ^{11}B a combination of the polarization effect and a direct covalent spin delocalization involving the ligand s and p orbitals appears necessary. A complete spin-polarized molecular orbital calculation on the $Np(BH_3CH_3)_4$ complex would be the most satisfactory way to explore the bonding in this molecule.

The Hyperfine Structure Anomaly for $^{241,239}Pu$ (32)

The hyperfine structure anomaly is defined as

$$\Delta = \frac{a_1 g_2}{a_2 g_1} - 1$$

where a_1 and a_2 are the hyperfine structure constants, and g_1 and g_2 are the nuclear g factors of two isotopes of the same element. This effect depends on the finite size of the nucleus and will be non-zero only for s and $p_{1/2}$ electrons which have a finite density at the nucleus. Relativistic effects increase the electron density at the nucleus which increases the magnitude of the hyperfine anomaly.

Bohr and Weisskopf (33), in their classic paper, give the following equation for the hyperfine anomaly:

$$\Delta \approx 0.3b \frac{g_S g_L}{g_S - g_L} \left(\frac{1}{g_I(1)} - \frac{1}{g_I(2)}\right)$$

where g_S, g_L, and g_I are the spin part, orbital part, and total nuclear g factors, respectively. The coefficient b has been evaluated from the calculations of Bohr and Weisskopf and their values for an s electron are shown in Figure 4. This coefficient arises from relativistic effects and is significant at large Z. Thus the magnitude of the hyperfine anomaly should be much larger in the actinide series than in the earlier part of the Periodic Table if the right pair of isotopes can be found and measured.

The above equation obtained from the Bohr-Weisskopf theory indicates that two isotopes which have much different nuclear moments (which is indicative of different nuclear ground states) could have a significant hyperfine anomaly. The nuclear magnetic moment of ^{239}Pu, I = 1/2 has been given as $^{239}\mu_N = +0.200 \pm 0.004$ nm (34). The value derived for ^{241}Pu, I = 5/2 is $^{241}\mu_N = -0.718 \pm 0.017$ nm.[1]

Two sets of high resolution optical transitions have been analyzed by Gerstenkorn and Tomkins for the isotopes ^{239}Pu and ^{241}Pu (35). The optical hyperfine structure constants given in Table 6 for the PuI level are assigned to the excited $^7D^0_1$ level. The transition is from the $5f^67s7p$ excited configuration to the ground $^7F_0$ level of the $5f^67s^2$ configuration (36). The second set of optical hyperfine structure constants is assigned to the ground $^8F_{1/2}$ level of PuII whose configuration is $5f^67s$ (37-38). The parent level ($^8G^0_{1/2}$) in this case is from the $5f^67p$ configuration. The observed hyperfine structure constants in these two levels are attributed to the 7s electron as the contribution from the $5f^6$ core (J = 0) is expected to be zero. There may be a contribution from the 7p level, but it is assumed this contribution to the ratio of the optical hyperfine coupling constants is small and can be neglected.

Analysis of the EPR data for Pu^{3+}/CaF_2 showed that the hyperfine structure constants in this case were due primarily to the $5f^5$ configuration (39) which means these hyperfine coupling constants are directly proportional to the corresponding nuclear magnetic moments. The optical and EPR data are shown in Table 6.

Assuming

$$\frac{A(^{241}Pu^{3+})I(^{241}Pu)}{A(^{239}Pu^{3+})I(^{239}Pu)} \approx \frac{g_I(^{241}Pu)}{g_I(^{239}Pu)}$$

then

$$^{241}\Delta^{239} = \frac{A(^{241}PuII)}{A(^{239}PuII)} \times \frac{A(^{239}Pu^{3+})}{A(^{241}Pu^{3+})} - 1 = -6.3 \pm .2\%.$$

From the Bohr-Weisskopf theory assuming $g_s = g$ (neutron), $g_L = Z/A$, and $b \approx 5.5\%$ (Figure 4), then

$$^{241}\Delta^{239} \approx -5.4\%$$

which agrees quite well with the experimental value.

The hyperfine structure anomaly for $^{239,241}Pu$ is quite large and represents a good example of a quantity whose magnitude depends on relativistic effects. In the actinide series, the hyperfine structure anomaly can be on the order of 1-10%, while for the lighter elements (isotopes) it usually is less than 1% (40).

Acknowledgement

I would like to thank Dr. Harry Dewey for helpful discussions and for sending me a draft of Ref. 12 prior to submission for publication.

I would also like to thank Dr. Earl Warden for helpful discussions about the PuI and PuII optical spectra.

This work was supported by the Director, Office of Energy Research, Office of Basic Energy Sciences, Chemical Sciences Division of the U.S. Department of Energy under Contract No. DE-AC03-76SF00098.

References

1. Katz, J.J.; Seaborg, G.T.; Morss, L.R., Ed., "The Chemistry of the Actinide Elements," 2nd Ed., Chapman and Hall: London, 1986.
2. Weinstock, B.; Malm, J.G. *J. Chem. Phys.* 1957, 27, 594.
3. Hutchison, C.A., Jr.; Tsang, T; Weinstock, B. *J. Chem. Phys.* 1962, 37, 555.
4. Hutchison, C.A., Jr.; Weinstock, B. *J. Chem. Phys.* 1960, 32, 56.
5. Butler, J.E.; Hutchison, C.A., Jr. *J. Chem. Phys.* 1981, 74, 3102.
6. Goodman, G.L.; Fred, M. *J. Chem. Phys.* 1959, 30, 849.
7. Eisenstein, J.C.; Pryce, M.H.L. *Proc. Roy. Soc. (London)* 1960, A255, 181.

8. Gruen, D.M.; Malm, J.G.; Weinstock, B. *J. Chem. Phys.* 1956, 24, 905.

9. Steindler, M.J.; Gunther, W.H. *Spectrochim. Acta* 1964, 20, 1319.

10. Kugel, R.; Williams, C.; Fred, M.; Malm, J.G.; Carnall, W.T.; Hindman, J.C. *J. Chem. Phys.* 1976, 65, 3486.

11. Dewey, H.J.; Barefield, J.E., II; Rice, W.W. *J. Chem. Phys.* 1986, 84, 684.

12. Mulford, R.N.; Dewey, H.J.; Barefield, J.E., II,to be submitted.

13. Koelling, D.D.; Ellis, D.E.; Bartlett, R.J. *J. Chem. Phys.* 1976, 65, 3331.

14. Boring, M.; Hecht, H.G. *J. Chem. Phys.* 1978, 69, 112.

15. Wadt, W.W. *J. Chem. Phys.* 1987, 86, 339.

16. Rajnak, K.; Gamp, E.; Shinomoto, R.; Edelstein, N. *J. Chem. Phys.* 1984, 80, 5942.

17. Van Deurzen, C.H.H.; Rajnak, K.; Conway, J.G. *J. Opt. Soc. Am. B* 1984, 1, 45.

18. Cowan, R.D. In "*The Theory of Atomic Structure and Spectra*," University of California Press: Berkeley, 1981, p. 214.

19. Flint, C.D.; Tanner, P.A. *Molec. Phys.* 1987, 61, 389.

20. Schlesinger, H.I.; Brown, H.C. *J. Am. Chem. Soc.* 1953, 75, 219.

21. Hoekstra, H.R.; Katz, J.J. *J. Am. Chem. Soc.* 1949, 71, 2488.

22. Banks, R.H.; Edelstein, N.M.; Rietz, R.R.; Templeton, D.H.; Zalkin, A. *J. Am. Chem. Soc.* 1978, 100, 1957.

23. Bernstein, E.R.; Keiderling, T.A. *J. Chem. Phys.* 1973, 59, 2105.

24. Rajnak, K.; Gamp, E.; Shinomoto, R.; Edelstein, N. *J. Chem. Phys.* 1984, 80, 5942.

25. Schlesinger, H.I.; Brown, H.C.; Horvitz, L.; Bond, A.C.; Tuck, L.D.; Walker, A.O. *J. Am. Chem. Soc.* 1953, 75, 222.

26. Shinomoto, R.; Gamp, E.; Edelstein, N.M.; Templeton, D.H.; Zalkin, A. *Inorg. Chem.* 1983, 22, 2351.

27. Rajnak, K.; Banks, R.H.; Gamp, E.; Edelstein, N. *J. Chem. Phys.* 1984, 80, 5951.

28. Kot, W. unpublished data.

29. Gamp, E.; Shinomoto, R.; Edelstein, N.; McGarvey, B.R. *Inorg. Chem.* 1987, 26, 2177.

30. Kurland, R.J.; McGarvey, B.R. *J. Magn. Reson.* 1970, 2, 286.

31. Baker, J.M. *J. Phys. C* 1968, 1, 1670.

32. Edelstein, N. *Phys. Letters* 1970, 33A, 233.

33. Bohr, A.; Weisskopf, V. *Phys. Rev.* 1950, 77, 94.

34. Faust, J.; Marrus, R.; Nierenberg, W.A. *Phys. Letters* 1965, 16, 71.

35. Gerstenkorn, S.; Tomkins, F.A. *Physica* 1969, 42, 581.

36. Blaise, J.; Fred, M.; Gutmacher, R.G. *J. Opt. Soc. Am. B* 1986, 3, 403.

37. Fred, M.; Blaise, J. In "*The Chemistry of the Actinide Elements,*" Katz, J.J.; Seaborg, G.T.; Morss, L.R., Eds., 2nd Ed.; Chapman and Hall: London, 1986, pp. 1196-1234.

38. The transition measured by Gerstenkorn and Tompkins (Ref. 35) was at 4536Å. In Ref. 35 the energy of this transition was given incorrectly and should be 22038.95 cm^{-1} (Ref. 37).

39. Edelstein, N.; Mehlhorn, R. *Phys. Rev. B* 1970, 2, 1225.

40. Fuller, G.H.; Cohen, V.W. "*A Table of Magnetic Hyperfine Anomalies,*" ORNL-4951, 1970.

$$b_4 = B_0^4/33, \quad b_6 = \left(\frac{-5}{429}\right) B_0^6$$

$$\theta = 8b_4 - 56b_6$$

$$\Delta = 10b_4 + 84b_6$$

Table 1. Correspondence between the crystal field parameters of Eq. 1 and the crystal field energy splittings of an f electron in the limit of zero spin-orbit coupling.

	Energy Experimental[a]	Energy This work[c]	Energy Ref. 7
Γ_7	0	0	0
Γ_8	7610	7610	7543
Γ_7'	9366[b]	9366	9348
Γ_8'		24891	24025
Γ_6		29310	28380

[a]Experimental data from Mulford, et al. (Ref. 12)

[b]The level at ~9350 cm^{-1} is split into two components and 9366 cm^{-1} is the major component. The splitting is attributed to Ar matrix effects. From Mulford, et al. Ref. 12.

[c]Calculated from parameters in column 2 of Table 3.

Table 2. Comparison of the energy levels of NpF_6 obtained from this analysis with that of Eisenstein and Pryce (Ref. 7) (in cm^{-1}).

	This work	Ref. 7
ζ	2409.9	2405.0
B_0^4	47967	45913.5
B_0^6	9279	8652.7

Table 3. Empirical parameters obtained from the optical spectrum and the ground state g value for NpF_6 (in cm^{-1}).

Parameter	U(V)[a,b]	$U(BD_4)_4/Hf(BD_4)_4$[a,c]	U(V)[d]	Pu(VII)[d]	$PuF_6(A)$[a,e]	$PuF_6(B)$[a,f]
F^2	51938(39)	41280(175)	76730	90662	35155(5174)	36026(2472)
F^4	42708(100)	40013(826)	50201	60062	72039(6964)	72458(3054)
F^6	27748(68)	22554(625)	36853	44390	38355(8123)	40535(3877)
ζ	1968(2)	1782(12)	2107	3123	2576(101)	2551(46)
α	35.5(0.4)	38(2)			[35.5]	[35.5]
β	-664(25)	[-648]			[-664]	[-664]
γ	744(26)	[1200]			[744]	[744]
P^2	573(66)	[500]			[573]	[573]
P^4	524(144)	[500]			[524]	[524]
P^6	1173(321)	[500]			[1173]	[1173]
B_0^4	-	-2445(124)			48172(1790)	48377(803)
B_0^6	-	-5371(81)			8728(400)	8690(180)
No. of levels	13	19			9	9
σ	9.8	53			117.8	54.2

[a]rms errors in ( ). Parameters in [ ] were held fixed. In all cases $M^0 = 0.987$, $M^2 = 0.550$, $M^4 = 0.384$.

[b]Ref. 17.

[c]Calc. B of Ref. 16.

[d]Results from the Hartree-Fock code of Cowan [Ref. 18].

[e]Assignments as given in Calc. A of Table 5. $E_{Ave} = 30551(763)$ cm^{-1}.

[f]Assignments of 2 Γ_3 and 2Γ_5 switched around from those used for Calc. A of Table 5. Parameters listed as Calc. B in Table 5. $E_{Ave} = 30669(349)$ cm^{-1}.

Table 4. Parameter values for various $5f^2$ ions (in cm^{-1}).

State	Experimental Values	Calc. A	Calc. B
1 Γ_{1g}	0.0	-17.2	6.1
1 Γ_{4g}	4582	4564	4552
1 Γ_{3g}	4554	4598	4579
1 Γ_{5g}	5130	5129	5124
2 $^{1}\Gamma_{4g}$	9764	9760	9748
2 Γ_{1g}	10467	10475	10476
2 Γ_{5g}	12114[a]	11999	12006
2 Γ_{3g}	11954[a]	12062	12079
3 Γ_{4g}	16256	16250	16251
3 Γ_{1g}		16659	16564
3 Γ_{5g}		18208	18433
3 Γ_{3g}		19656	19707
4 Γ_{3g}		21114	21092
4 Γ_{4g}		21394	21398
4 Γ_{5g}		23360	23343
1 Γ_{2g}		25409	25344

[a]The assignments of these two levels were switched in the fit that resulted in the energy levels listed under calculation B.

Table 5. Experimental and Calculated Energy Levels of PuF_6 (in cm^{-1}).

k^a	g_{Γ_6}	g_{exp}
1.0	2.377	
0.885	1.896	1.896 [$Np(BD_4)_4$]
0.862	1.799	1.799[$Np(BH_3CH_3)_4$]

$^a g = \langle\psi\|k\,\mathbf{L} + g_s\,\mathbf{S}\|\psi\rangle$.

Table 6. Calculated and experimental values for the ground-state g value (g_{Γ_6}) for $Np(BD_4)_4$ and $Np(BH_3CH_3)_4$. From Ref. 27.

	H_b	H_{CH_3}	B
K (MHz)	-5.165	-0.495	-3.116
Std. dev. (ppm)	2.4	0.24	7.48

Table 7. Best-fit values of the hyperfine parameter, K for $Np(BH_3CH_3)_4$ calculated with an orbital reduction factor of 0.862.

Ion	Level (cm^{-1})	A ($10^{-3}cm^{-1}$)	$\frac{A(^{241}Pu)I(^{241}Pu)}{A(^{239}Pu)I(^{239}Pu)}$	Ref.
^{241}Pu I	23766	-58.25 ± 0.2	-3.367 ± 0.02	35
^{239}Pu I	23766	86.5 ± 0.2		
^{241}Pu II	0	-167.3 ± 0.5	-3.362 ± 0.02	35
^{239}Pu II	0	248.8 ± 0.5		
$^{241}Pu^{3+}$	0	|4.807| ± 0.010	|3.590| ± 0.010	32
$^{239}Pu^{3+}$	0	|6.695| ± 0.003		

Table 8. Hfs constants for various levels of Pu ions.

Figure Captions

Figure 1. Relative energy levels of one f electron subject to spin-orbit coupling and an octahedral crystalline field. The energy levels are drawn as a function of the relative strengths of the two interactions assuming $B_0^6 = 0$ with $E_o = [(\frac{7\zeta}{2})^2 + (18b_4)^2]^{1/2}$ and $\chi = x/1+x$ where $x = \left|\frac{7\zeta}{2}/18b4\right|$.

Figure 2. Comparison of the calculated $1/\chi$ vs. temperature curve for NpF_6 with some of the experimental data of Reference 4.

Figure 3. T^{-1} dependence of the paramagnetic shifts for ^1H and ^{11}B for $Np(BH_3CH_3)_4$. All shifts are to lower fields. The solid lines are calculated from Eq. 3 in the text.

Figure 4. Plot of the coefficient b vs atomic number. The calculated points have been taken from Ref. 33. The dotted line represents a polynomial fit to the calculated points extrapolated to Z = 100.

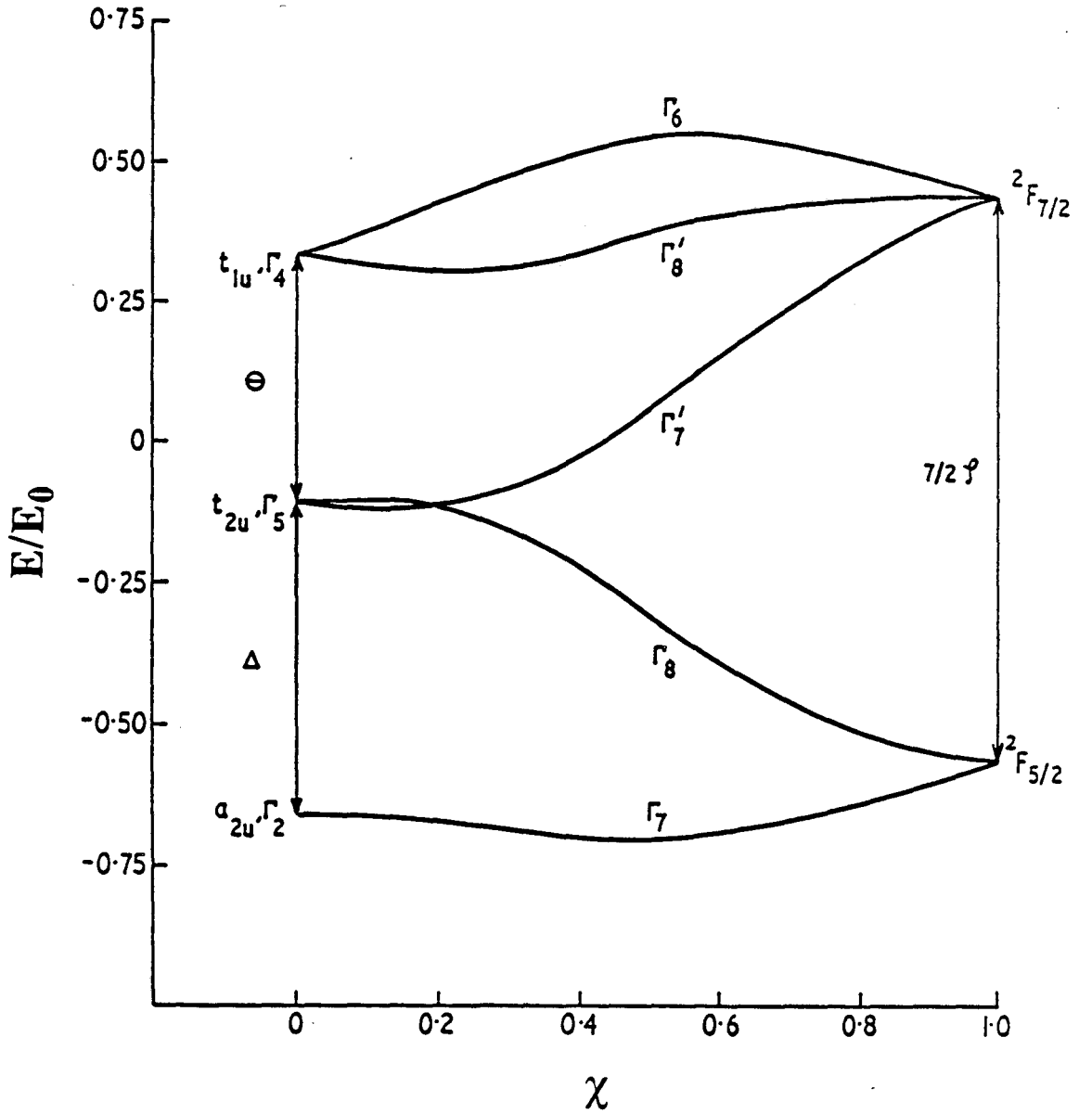
0·75
0·50
0·25
0
-0·25
-0·50
-0·75
E/E0
Γ6
2F7/2
t1u,Γ4
Γ'8
Θ
Γ'7
7/2 ζ
t2u,Γ5
Δ
Γ8
2F5/2
a2u,Γ2
Γ7
0
0·2
0·4
0·6
0·8
1·0
χ

Figure 1

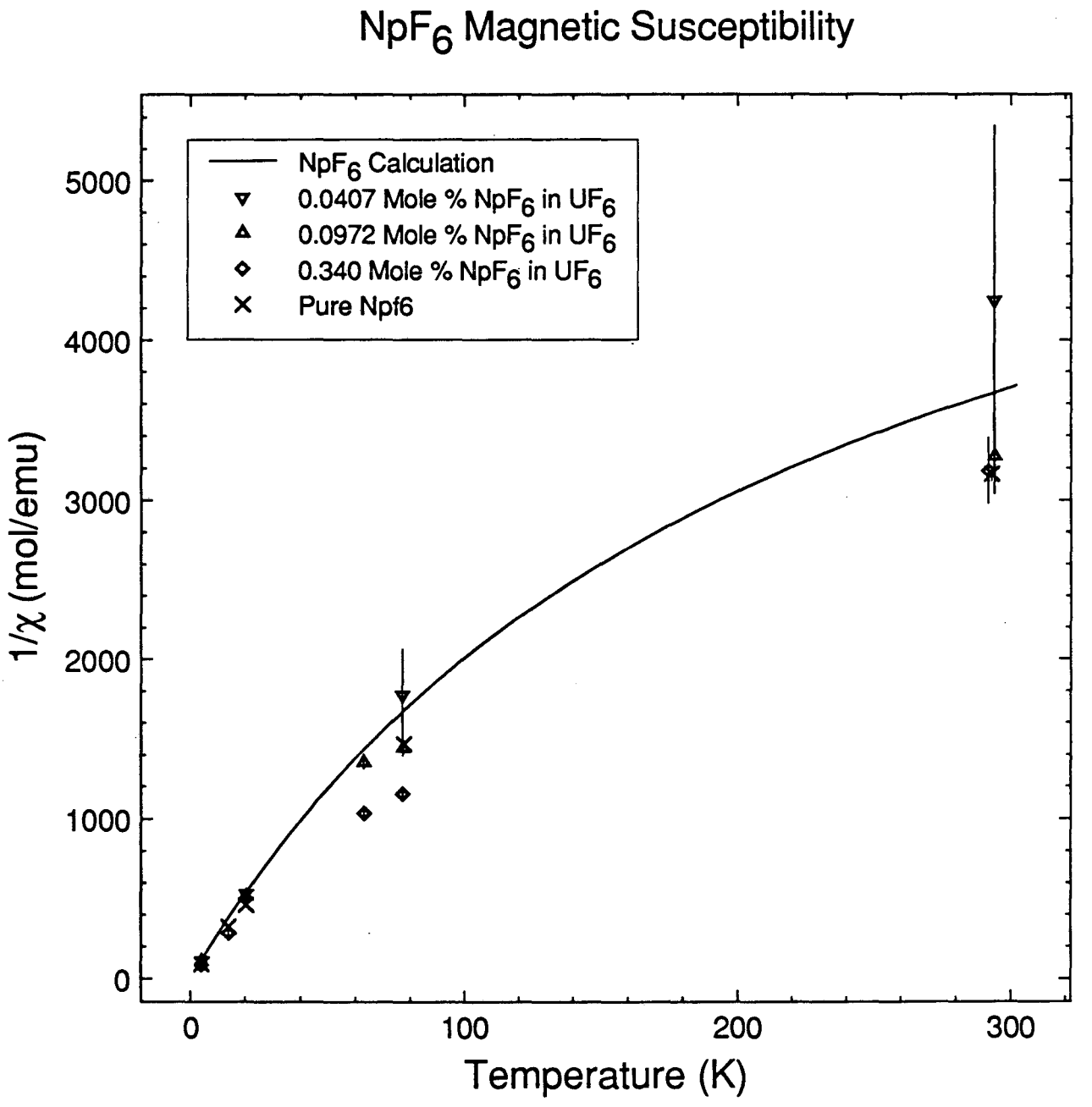
NpF6 Magnetic Susceptibility
NpF6 Calculation
0.0407 Mole % NpF6 in UF6
0.0972 Mole % NpF6 in UF6
0.340 Mole % NpF6 in UF6
Pure Npf6
1/χ (mol/emu)
5000
4000
3000
2000
1000
0
0
100
200
300
Temperature (K)

Figure 2

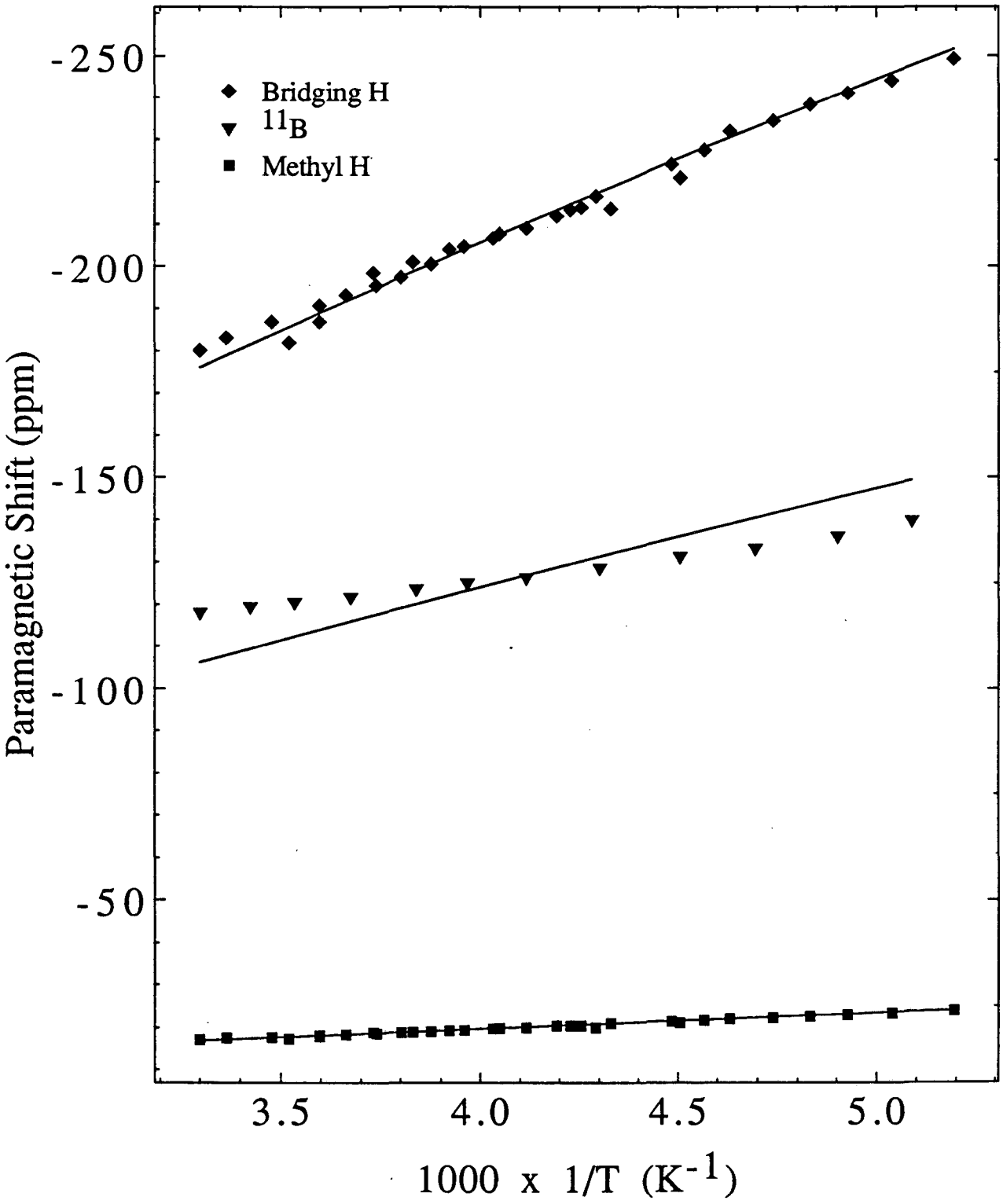
Bridging H
11B
Methyl H
-250
-200
-150
-100
-50
Paramagnetic Shift (ppm)
3.5
4.0
4.5
5.0
1000 x 1/T (K-1)

Figure 3

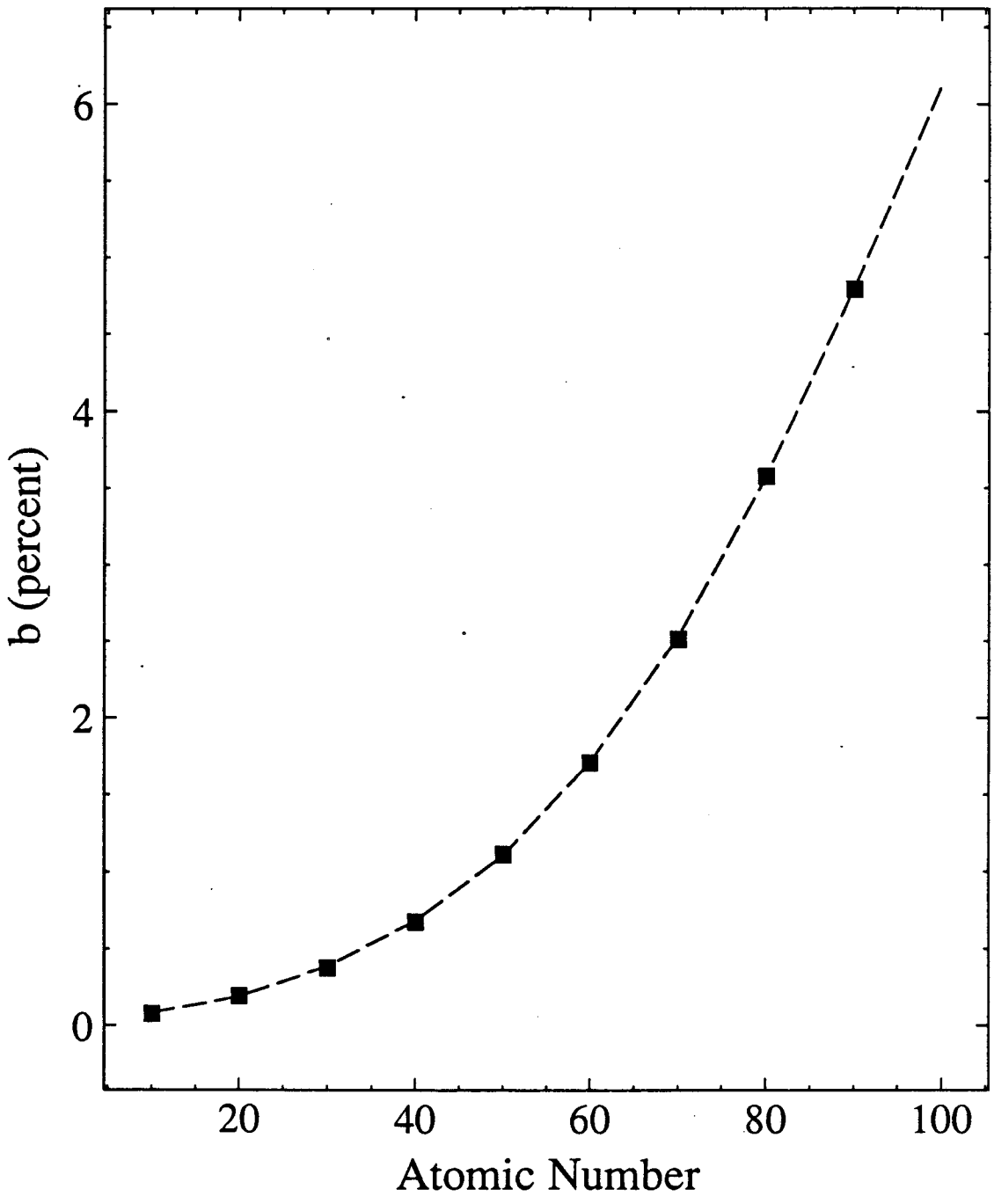

Figure 4

LAWRENCE BERKELEY LABORATORY
UNIVERSITY OF CALIFORNIA
INFORMATION RESOURCES DEPARTMENT
BERKELEY, CALIFORNIA 94720